Electronic Supplementary Material (ESI) for ChemComm.

L-proline, a resolution agent able to target both enantiomers of mandelic acid: an exciting case of stoichiometry controlled chiral resolution.

Fuli Zhou, Laurent Collard, Koen Robeyns, Tom Leyssens, Oleksii Shemchuk

Institute of Condensed Matter and Nanosciences, UCLouvain, 1 Place Louis Pasteur, B-1348 Louvain-la-Neuve, Belgium

Table of Contents

EXPERIMENTAL PART

Materials and instrumentation

All reagents were purchased from either Merck or TCI Chemicals and used without further purification.

Solid-state synthesis

Cocrystallization experiments were performed via neat grinding. R-MAN·L-PRO, S-MAN·L-PRO, and S-MAN·L-PRO_2 were obtained by grinding stoichiometric quantities of enantiopure (0.3 mmol) mandelic acid with L-proline (0.3 or 0.6 mmol) using a "Retsch Mixer Mill MM 400" equipped with two grinding jars each able to contain five Eppendorf tubes of 2 mL. Besides the reagents, each tube was filled with three small stainless-steel beads. Grinding was performed at 30 Hz for 90 minutes.

Solution synthesis

Single crystals of R-MAN·L-PRO and S-MAN·L-PRO were obtained by slow evaporation at RT from undersaturated methanol solutions (2 mL) of equimolar quantities of the corresponding reagents (0.3 mmol). S-MAN·L-PRO_2 was obtained following the same procedure but using the corresponding stoichiometric ratio (0.3-0.6 mmol).

Slurry experiments

The slurry experiments used to screen for an appropriate solvent (table ESI-3), and to construct the isoplethal ternary diagrams in ethanol (tables ESI-5 and ESI-6) were constructed as follows. In a 2 ml glass vial, a given amount of solvent, a given quantity of RS-mandelic acid and L-proline were added (see tables for the specific quantities). The obtained vials were sealed and stirred at 700 rpm for 3 days at 25°C using a Cooling Thermomixer HLC. After 12h of stirring, each vial was seeded with traces of all possible solid forms (both parent compounds and all possible cocrystals). After 3 days, the equilibrium was assumed to be reached, and the powders were filtered, washed, dried, and analysed using XRPD.

The scale-up conditions used for the resolution of both enantiomers are as follows:

RL: 0.69 g of RS-mandelic acid and 2.13 g of L-proline were slurried in 6.5 mL of ethanol in a sealed 20 mL vial at 750 rpm for 48 hours at RT. The suspension was filtered and the solid phase was dried, washed and analysed using XRPD.

SL_2: 1.654 g of RS-mandelic acid and 2.95 g of L-proline were suspended in 30 mL of ethanol in a 100 mL Erlenmeyer flask. The flask was sealed and stirred at 500 rpm for 2 weeks at RT. Afterwards, the powder was filtered, dried and characterized using XRPD. The powder was shown to correspond to the expected **SL_2 + L-proline** mixture (fig. ESI-8).

Cocrystals dissociation in separate components

Both cocrystals were separated into components following similar procedures. 1.5 g of **SL_2** was suspended in 20 mL of ethyl ether for 24h. The suspension was filtered, and the solid material was analysed by XRPD showing pure L-proline. The mother liquor obtained after filtration was left to evaporate. The solid obtained was slurried in 10mL of chloroform for 24h. The suspension was filtered and the recovered mother liquor was left to evaporate. The

obtained solid was analysed by XRPD showing pure S-mandelic acid. As for the **RL** cocrystal, 5g were initially suspended in 50mL of diethyl ether and then in 25mL of chloroform.

Single Crystal X-ray Diffraction

Single crystals were grown starting with enantiopure compounds allowing attribution of absolute configuration. The single crystals of all three cocrystals described in this manuscript (RL, SL and SL2) were obtained by recrystallization of the corresponding powders in the undersaturated methanol solution. Approximately 30 mg of each cocrystal obtained in the corresponding ball milling experiment (R+L, S+L and S+2L) were dissolved in 5 mL of methanol and left to evaporate at RT. Single crystal X-ray diffraction (SCXRD) data were collected on a MAR345 image plate detector using Mo Kα radiation (λ = 0.71073 Å), generated by an Incoatec IμS microfocus source. Data integration and reduction was performed by CrystAlis^{PRO} and the implemented absorption correction was applied. Structure solution was performed by the dual-space algorithm in SHELXT and the structure was further refined against F^2 using SHELXL.[2] Non-hydrogen atoms were refined anisotropically; H_{CH} atoms were added in calculated positions; H_{OH} and H_{NH} atoms were either located from a Fourier map or added in calculated positions and refined riding on their respective carbon, nitrogen or oxygen atoms. Symmetry analysis and validation were carried out using PLATON.[3] Figures were made using the molecular visualization software Mercury v4.3.[4] CCDC 2174324-2174326 contain the supplementary crystallographic data for this paper. These data can be obtained free of charge from The Cambridge Crystallographic Data Centre via www.ccdc.cam.ac.uk/structures.

Powder X-ray Diffraction

For phase identification purposes, room temperature X-ray powder diffraction (XRPD) patterns were collected on a PANalytical Bragg-Brentano diffractometer, using Ni-filtered CuKα (λ = 1.54179 Å) at 45 kV and 30 mA with a X'Celerator detector. Each sample was analyzed between 4 and 40° in 2θ with a step size of ca. 0.0167° and a total scan time of 6min42s.

Alternatively, XRPD measurements were performed with a Siemens D5000 diffractometer equipped with a Cu X-ray source operating at 40kV and 40 mA and a secondary monochromator allowing to select the Kα radiation of Cu (λ = 1.5418 Å). A scanning range of 2θ values from 5° to 50° at a scan rate of 0.6° min^{-1} was applied.

Chiral High-Performance Liquid Chromatography (cHPLC)

The separation of *R*-/*S*-mandelic acid was performed by Chiral HPLC using a Waters Alliance 2695 coupled with a PDA996 detector. The mandelic acid enantiomers were separated on a Daicel Chiralpak IC column 4.6x250mm 5µm with a mix of 95% v/v i-hexane, 5% v/v Isopropanol and 0.1% of TFA as mobile phase. The flow rate used in this method was 1mL/min at 25°C and the data was extracted at a wavelength of 205 nm.

EXPERIMENTAL RESULTS

Crystallographic data

Table ESI-1. Crystal data and structure refinement for **RL**, **SL** and **SL_2**.

Identification code	**R-MAN·L-PRO (RL)**	**S-MAN·L-PRO (SL)**	**S-MAN·(L-PRO)$_2$ (SL_2)**
Empirical formula	C13 H17 N O5	C13 H17 N O5	C18 H26 N2 O7
Formula weight / g·mol^{-1}	267.27	267.27	382.41
Temperature / K	297(2)	297(2)	297(2)
Crystal system	Orthorhombic	Monoclinic	Monoclinic
Space group	$P2_12_12_1$	$P2_1$	$P2_1$
a / Å	7.8248(5)	14.6468(7)	5.9617(14)
b / Å	7.9556(4)	5.7771(2)	9.3791(15)
c / Å	20.9680(11)	16.2043(9)	16.778(3)
α / °	90	90	90
β / °	90	107.386(6)	90.189(19)
γ / °	90	90	90
Volume / Å^3	1305.28(12)	1308.50(12)	938.1(3)
Z	4	4	2
Density (calculated) / g·cm^{-3}	1.360	1.357	1.354
Absorption coefficient / mm^{-1}	0.105	0.105	0.104
F(000)	568	568	408
Crystal size / mm^3	0.19 x 0.18 x 0.15	0.28 x 0.08 x 0.05	0.15 x 0.12 x 0.01
θ range for data collection / °	3.214 to 26.091	2.817 to 25.349	3.258 to 21.961
Reflections collected	9519	9623	4164
Independent reflections	2586 [$R_{(int)}$ = 0.0326]	4725 [$R_{(int)}$ = 0.0361]	4164 [$R_{(int)}$ = 0.037]
Completeness to θ = 25.242° / %	99.5	99.5	99.5
Data / restraints / parameters	2586 / 0 / 174	4725 / 54 / 357	4164 / 373 / 373
Goodness-of-fit on F^2	1.092	1.074	1.096
Final R indices [I>2sigma(I)]	R_1 = 0.0444, wR_2 = 0.1134	R_1 = 0.0443, wR2 = 0.0961	R_1 = 0.0769, wR_2 = 0.1903
R indices (all data)	R_1 = 0.0535, wR_2 = 0.1205	R_1 = 0.0631, wR2 = 0.1027	R_1 = 0.1322, wR_2 = 0.2162

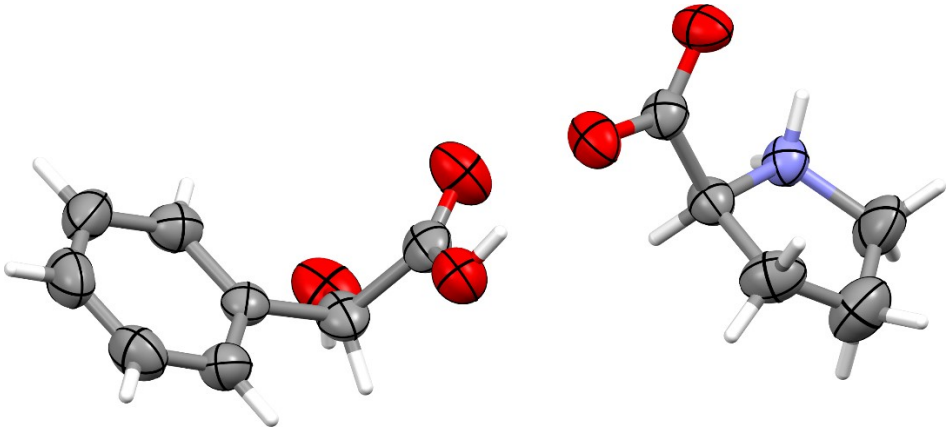

Figure ESI-1. ORTEP representation of **RL** with displacement ellipsoids drawn at the 50% probability level. Hydrogen atoms are shown as capped sticks for clarity.

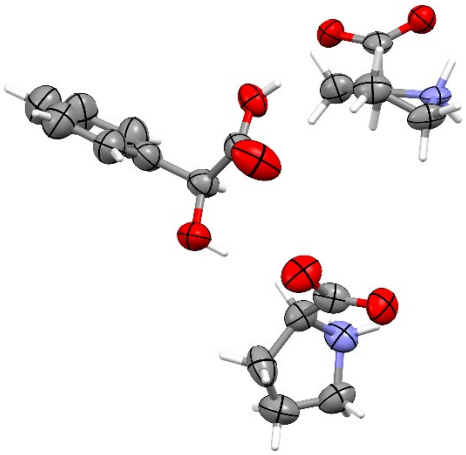

Figure ESI-2. ORTEP representation of **SL2** with displacement ellipsoids drawn at the 50% probability level. Hydrogen atoms are shown as capped sticks and the minor disordered part was removed for clarity.

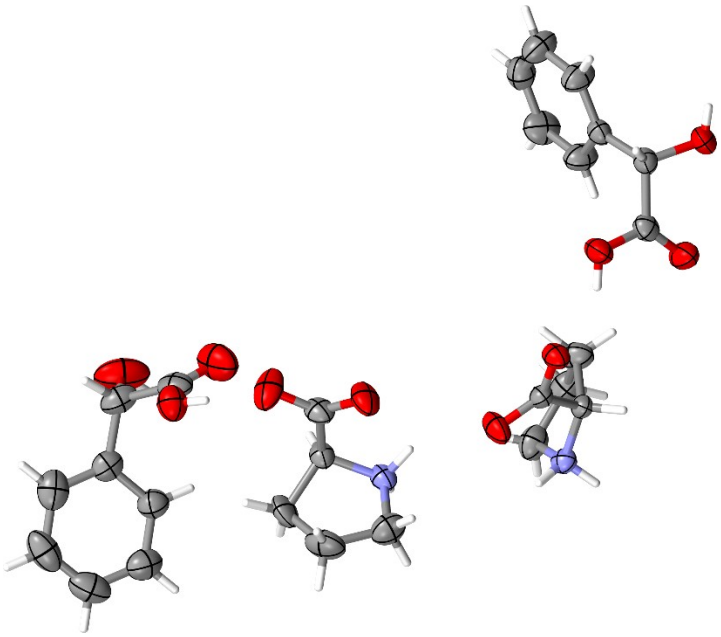

Figure ESI-3. ORTEP representation of **SL** with displacement ellipsoids drawn at the 50% probability level. Hydrogen atoms are shown as capped sticks and the minor disordered part was removed for clarity.

XRPD patterns

All the experimental patterns shown in this section were obtained mechanochemically according to the equations of scheme 2 (see Experimental part).

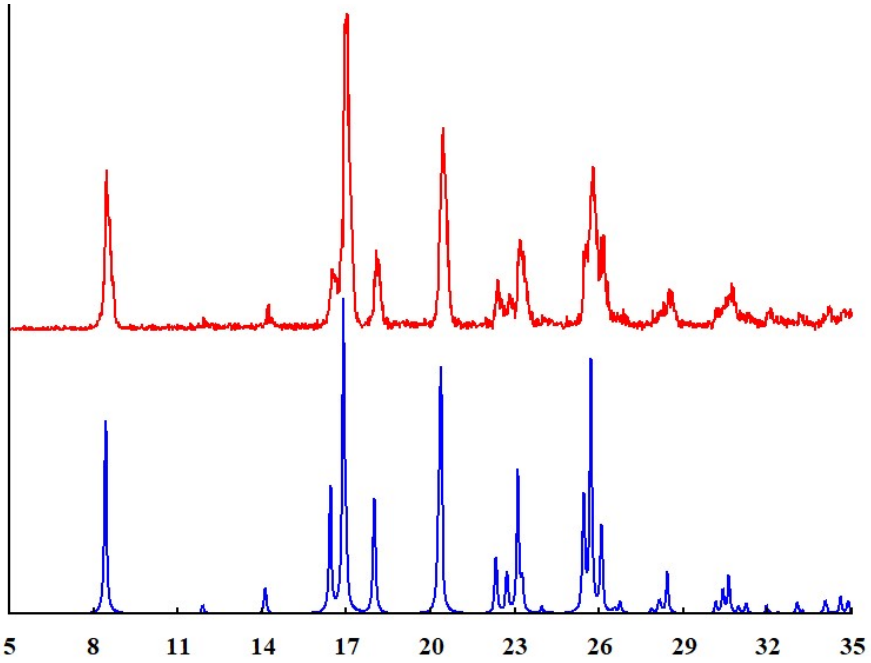

Figure ESI-4. Comparison between the experimental (red) and calculated (blue) XRPD patterns for **RL**.

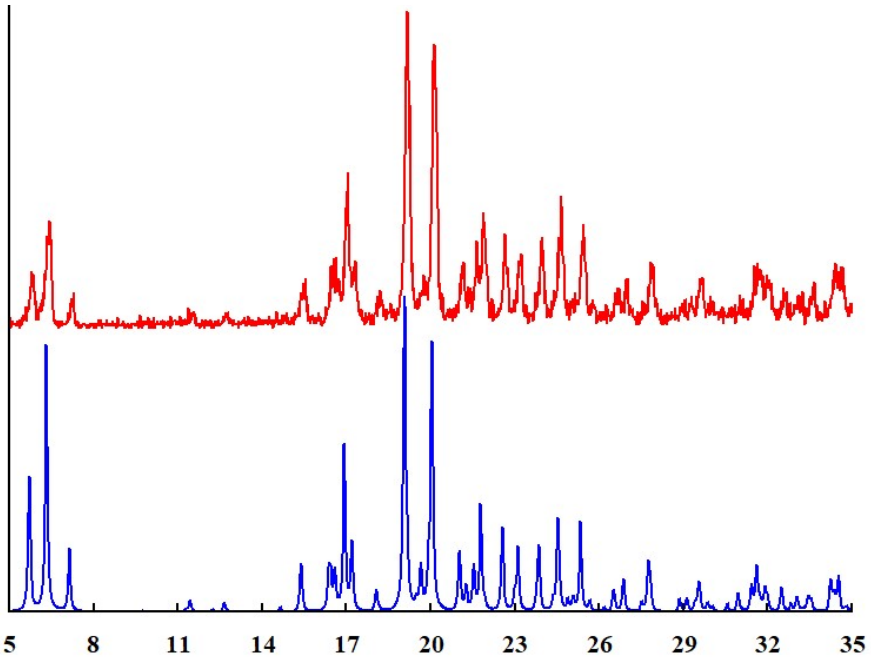

Figure ESI-5. Comparison between the experimental (red) and calculated (blue) XRPD patterns for **SL**.

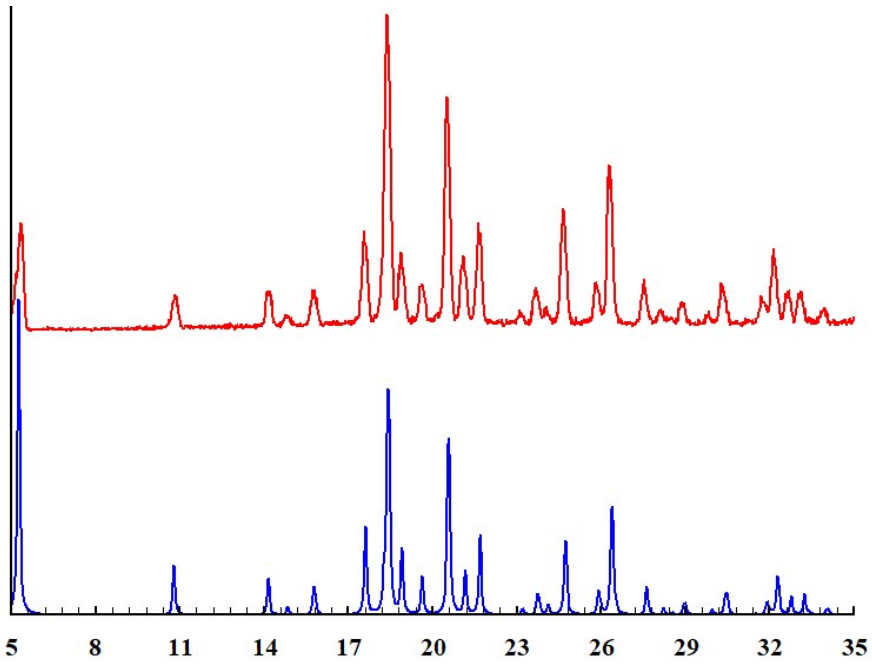

Figure ESI-6. Comparison between the experimental (red) and calculated (blue) XRPD patterns for **SL_2**.

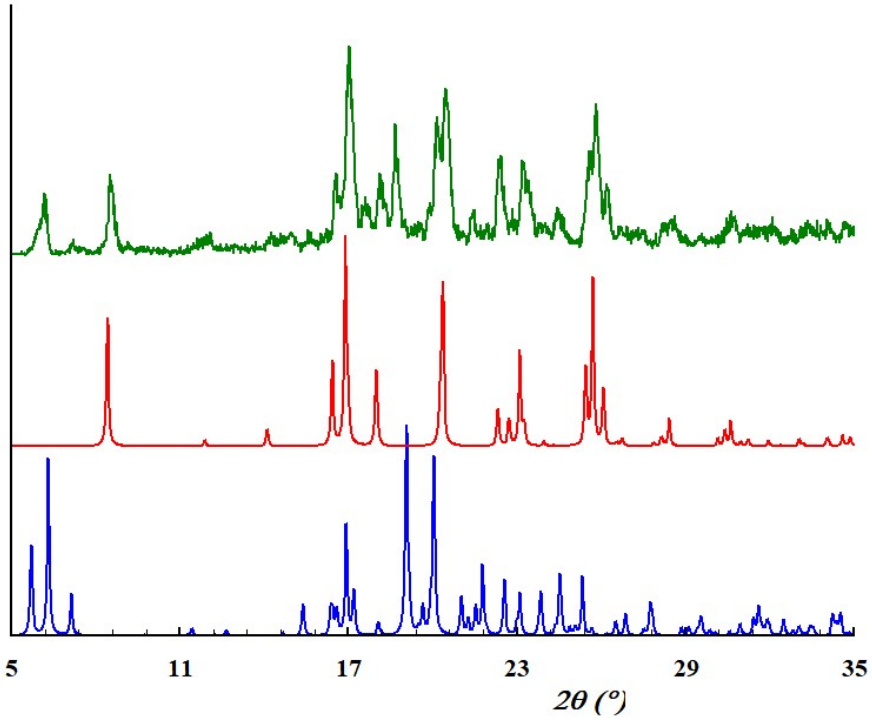

Figure ESI-7. Comparison between experimental grinding outcome of RS-mandelic acid with L-proline (green) with the calculated patterns of **RL** (red) and **SL** (blue) – a diastereomeric mixture.

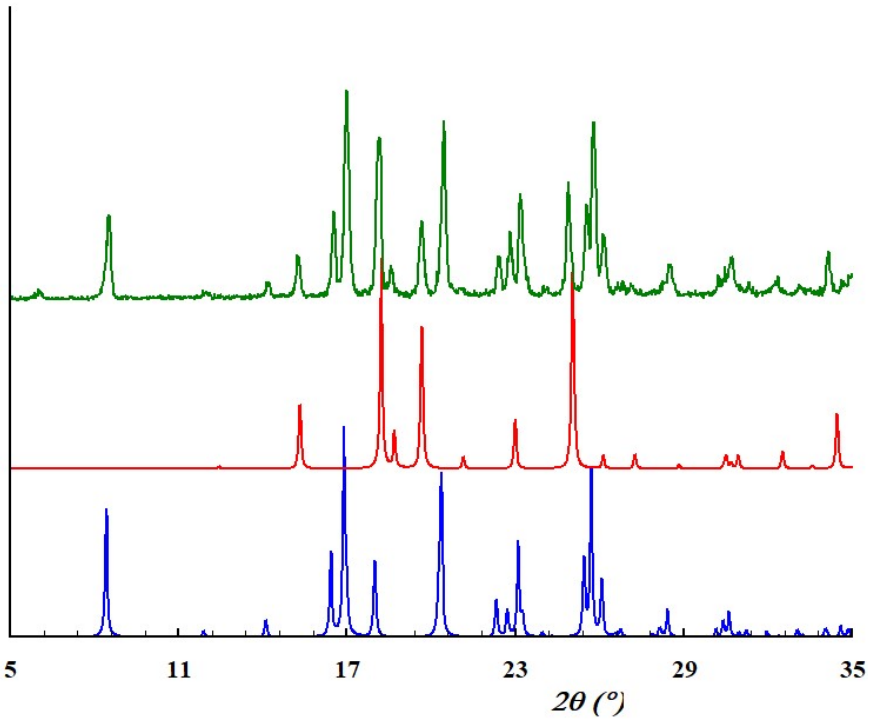

Figure ESI-8. Comparison between experimental grinding outcome of R-mandelic acid with 2 equivalents of L-proline (green) with the calculated patterns of **RL** (blue) and L-proline (red). Tiny traces of the unreacted R-mandelic acid are present.

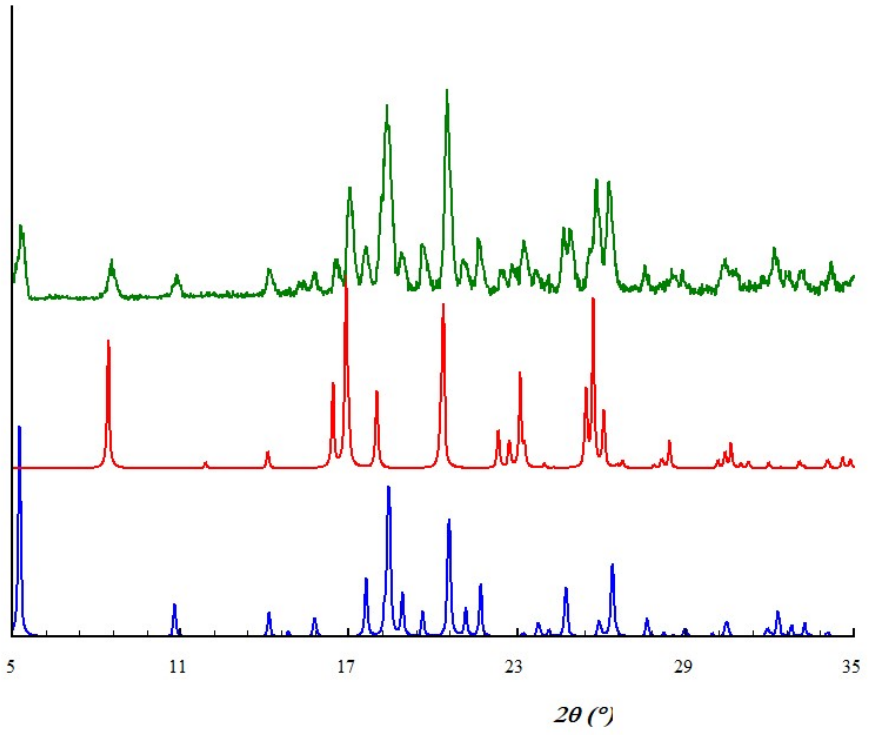

Figure ESI-9. Comparison between experimental grinding outcome of RS-mandelic acid with 2 equivalents of L-proline (green) with the calculated patterns of **RL** (red) and **SL_2** (blue). Traces of unreacted L-proline are present in the experimental XRPD pattern.

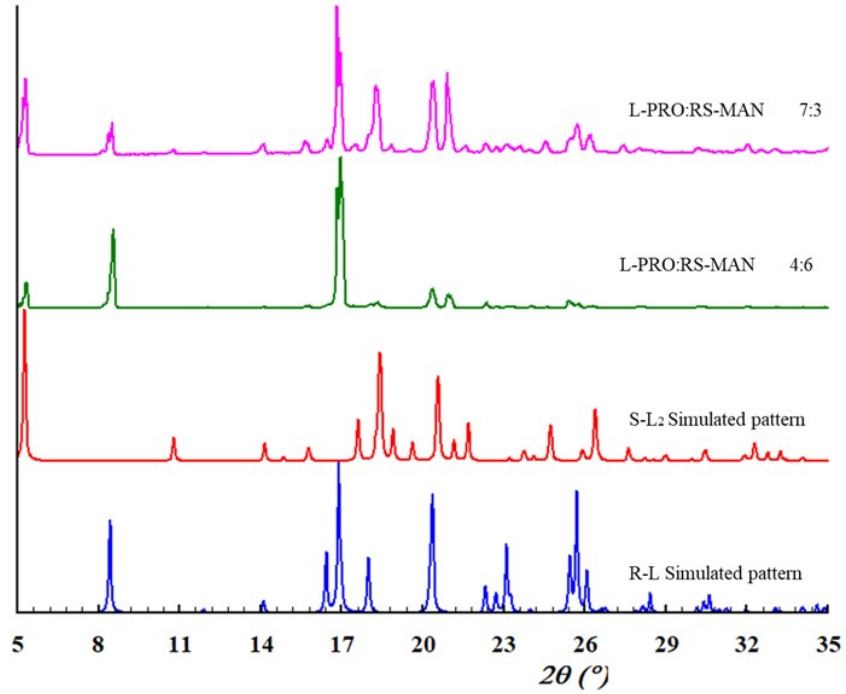

Figure ESI-10. Comparison between slurry outcome of L-proline and RS-mandelic acid in 7:3 (pink) and 4:6 (green) ratios. The simulated patterns of **SL_2** (red) and **RL** (blue) are shown for comparison.

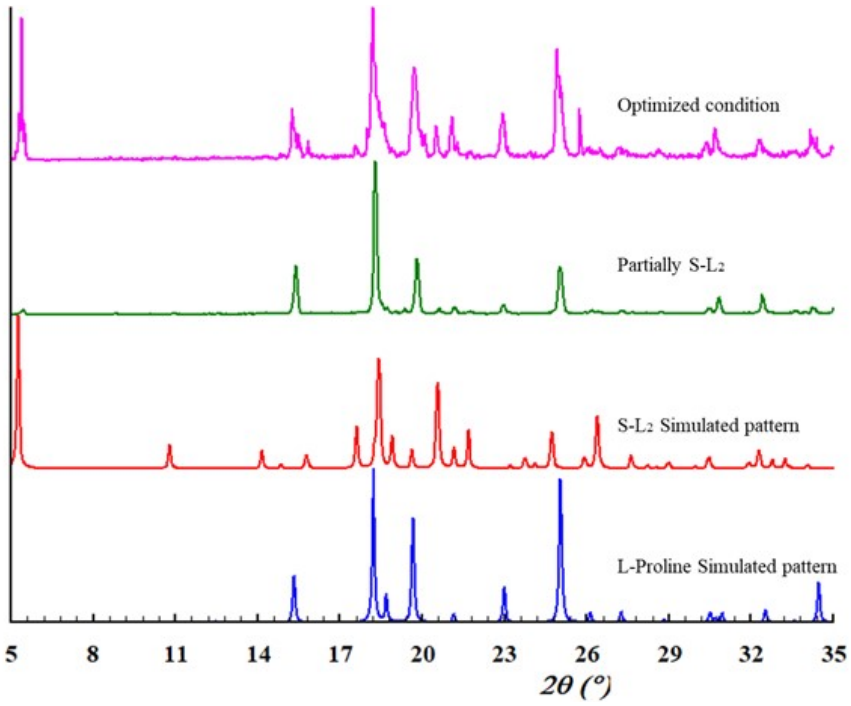

Figure ESI-11. Comparison between slurry outcome of L-proline and RS-mandelic acid (289.8 mg of L-proline, 163.8 mg of RS-mandelic acid in 3.0 g of ethanol – green) with the optimized reaction conditions (272mg L-proline, 163.8 mg of RS-mandelic acid in 3.0 g ethanol – pink). The simulated patterns of **SL_2** (red) and **L-proline** (blue) are shown for comparison.

Solid-state grinding experiments

To explore the reactions shown in scheme 2, as well as to create the solid-state ternary diagram a series of neat grinding experiments was performed. Table 2 shows the reaction outcomes.

Table ESI-2. Experimental data for system of *R*-mandelic acid*: S*-mandelic acid : L-proline at solid-state.

Reagents		Mandelic acid : L-proline (mole ratio)	Mass (mg)		Resultant XRPD
			Mandelic acid	L-proline	
R-mandelic acid	**L-proline**	1:1	45.6	34.5	**RL**
S-mandelic acid	**L-proline**	1:1	45.6	34.5	**SL**
RS-mandelic acid	**L-proline**	1:1	45.6	34.5	**RL + SL**
R-mandelic acid	**L-proline**	1:2	45.6	69	**RL + L-pro**
S-mandelic acid	**L-proline**	1:2	45.6	69	**SL_2**
RS-mandelic acid	**L-proline**	1:2	45.6	69	**RL + SL_2 + L-pro**
R-mandelic acid	**L-proline**	2:1	91.2	34.5	**R + RL**
S-mandelic acid	**L-proline**	2:1	91.2	34.5	**S + SL**
RS-mandelic acid	**L-proline**	2:1	91.2	34.5	**RL+SL_2**

Solvent screening

The most promising solvent was selected based on preliminary slurry experiments. To this extent, we performed a series of thermodynamic suspension experiments in 9 different solvents, varying the overall composition in racemic mandelic acid *vs* L-Proline (Table ESI-3). To make sure thermodynamic equilibrium was reached, vials were seeded with all possible solid forms encountered in this work.

The solubility in water and methanol is relatively high, leading to undersaturated solutions for the overall concentrations used here. Given the right conditions, **RL** can be obtained as the only stable phase in suspension as shown by the slurry in ethanol using a 2:1 mandelic acid-Proline ratio. In no instance, did we observe a suspension of **RL** and **SL** cocrystals. Interestingly, for all solvents, combinations of **RL** with the **SL_2** cocrystal could be obtained, as only two solids, or in combination with racemic mandelic acid, or L-Proline depending on the amount of amino acid used.

Table ESI-3. Suspension outcome (XRPD) for various ratios of RS-mandelic acid – L-proline (300 mg of total weight) in different solvents (2mL) at a temperature of 25°C.

Ratio / Solvent	2:1	1:1	1:2	1:4
H_2O	Dissolved	Dissolved	Dissolved	Dissolved
Methanol	Dissolved	Dissolved	Dissolved	Dissolved
Ethanol	**RL**	**RL + SL_2**	**RL + SL_2 + L-pro**	**L-pro**
Acetone	**RL + SL_2**	**RL + SL_2**	**RL + SL_2 + L-pro**	**RL + SL_2 + L-pro**
Acetonitrile	**RS-man + RL**	**RS-man + RL + SL_2**	**RL + SL_2 + L-pro**	**RL + SL_2 + L-pro**
Chloroform	**RS-man + RL**	**RS-man + RL + SL_2**	**RL + SL_2 + L-pro**	**RL + SL_2 + L-pro**
Nitromethane	**RS-man + RL**	**RS-man + RL + SL_2**	**RL + SL_2 + L-pro**	**RL + SL_2 + L-pro**
Ethyl acetate	**RL + SL_2**	**RL + SL_2**	**RL + SL_2 + L-pro**	**RL + SL_2 + L-pro**
Toluene	**RS-man + RL + SL_2**	**RL + SL_2**	**RL + SL_2 + L-pro**	**RL + SL_2 + L-pro**

Isoplethal ternary phase diagram data points

Table ESI-4. Experimental Data for System of L-proline : RS-mandelic acid : EtOH at 298 K.

Initial composition L-proline : RS-mandelic acid (mol%)	Initial components (mg)			Initial components (mol %)			Solid phase at equilibrium
	L-proline	RS-mandelic acid	EtOH	L-proline	RS-mandelic acid	EtOH	
0:100	0	760	251	0.00	47.83	52.17	**RS-man**
5:95	28.75	722	214	2.59	49.22	48.19	**RS-man**
10:90	57.5	684	200	5.35	48.15	46.50	**RS-man**
15:85	86.2	646	200	8.02	45.48	46.50	**RS-man**
20:80	57.5	303.4	300	5.55	22.14	72.31	**RL**
25:75	57.2	228	500	3.87	11.66	84.47	**RL**
30:70	69	212.8	500	4.66	10.88	84.45	**RL**
35:65	80.45	197.6	500	5.44	10.11	84.46	**RL**
40:60	92	182.4	1310	2.63	3.94	93.44	**RL + SL_2**
45:55	103.5	166.2	860	4.35	5.29	90.36	**RL + SL_2**
50:50	105	152	830	4.58	5.01	90.41	**RL + SL_2**
55:45	84.2	91.2	476	6.27	5.14	88.59	**RL + SL_2**
60:40	132.1	109.8	400	10.87	6.84	82.29	**RL + SL_2**
65:35	111.9	79.8	925	4.51	2.43	93.06	**RL + SL_2**
70:30	144.9	81.9	900	5.90	2.52	91.58	**RL + SL_2**
75:25	129	57	430	10.35	3.46	86.19	**RL + SL_2**
80:20	147.2	48	440	11.47	2.83	85.70	**RL + SL_2 + L-pro**
85:15	80	18	437	6.75	1.15	92.10	**L-pro**
90:10	82	12	451	6.73	0.75	92.52	**L-pro**
95:5	66	6	400	6.17	0.42	93.41	**L-pro**
100:0	22	0	670	1.30	0.00	98.70	**L-pro**

Table ESI-5. Experimental Data for System of *RS*-mandelic acid :L-proline : EtOH at 298 K.

Initial composition L-Proline : RS-Mandelic acid (%)	Initial components (mg)			Initial components (mol %)			Solid phase at equilibrium
	L-proline	RS-mandelic acid	EtOH	L-proline	RS-mandelic acid	EtOH	
65:35	223.8	159.6	2400	3.53	1.90	94.57	**RL + SL_2 + L-pro**
65:35	223.8	159.6	2700	3.16	1.70	95.14	**RL + SL_2 + L-pro**
65:35	223.8	159.6	3000	2.85	1.54	95.61	**L-pro**
65:35	223.8	159.6	3700	2.33	1.26	96.41	**L-pro**
65:35	223.8	159.6	4900	1.78	0.96	97.26	**L-pro**
70:30	289.8	163.8	2400	4.52	1.93	93.55	**RL + SL_2 + L-pro**
70:30	289.8	163.8	2700	4.05	1.73	94.22	**RL + SL_2 + L-pro**
70:30	289.8	163.8	3000	3.66	1.57	94.77	**SL_2 + L-pro**
70:30	289.8	163.8	3700	3.00	1.28	95.72	**L-pro**
70:30	289.8	163.8	4900	2.29	0.98	96.73	**L-pro**
75:25	258	114	2400	4.07	1.36	94.57	**SL_2 + L-pro**
75:25	258	114	2700	3.64	1.22	95.15	**L-pro**
75:25	258	114	3000	3.29	1.10	95.61	**L-pro**
75:25	258	114	3700	2.69	0.90	96.41	**L-pro**
75:25	258	114	4900	2.05	0.69	97.27	**L-pro**

Chiral High Performance Liquid Chromatography

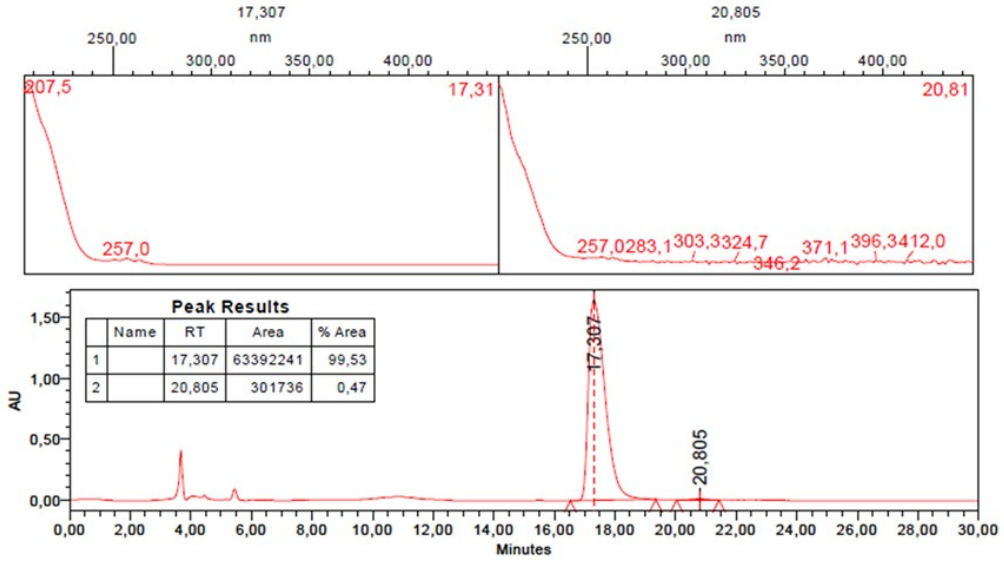

Figure ESI-12. HPLC chromatograms used to determine the R-MAN/S-MAN concentration after dissociation of the **RL** cocrystal according to the procedure mentioned above (*ee* >99%).

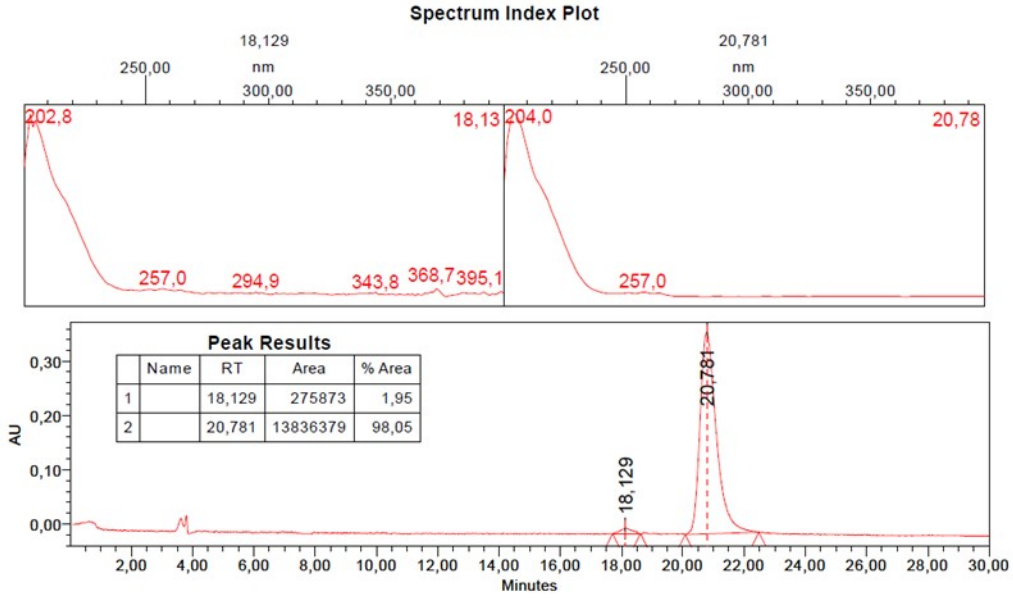

Figure ESI-13 HPLC chromatograms used to determine the R-MAN/S-MAN ratio after dissociation of the **SL_2** cocrystal according to the procedure mentioned above (*ee* >96.1%).

References

(1) Rigaku, O. D., CrysAlisPro Software System, Version 1.171. 38.41 l, Rigaku Coorporation. In ed.; Oxford, UK: 2015.
(2) Sheldrick, G. M., Crystal structure refinement with SHELXL. *Acta Crystallogr C Struct Chem* **2015,** 71, (Pt 1), 3-8.
(3) Spek, A. L., Structure validation in chemical crystallography. *Acta Crystallogr D Biol Crystallogr* **2009,** 65, (Pt 2), 148-55.
(4) Macrae, C. F.; Bruno, I. J.; Chisholm, J. A.; Edgington, P. R.; McCabe, P.; Pidcock, E.; Rodriguez-Monge, L.; Taylor, R.; Streek, J. v. d.; Wood, P. A., Mercury CSD 2.0–new features for the visualization and investigation of crystal structures. *Journal of Applied Crystallography* **2008,** 41, (2), 466-470.